

Positive and negative electrocaloric effect in BaTiO_3 in the presence of defect dipoles

Yang-Bin Ma,^{1, a)} Karsten Albe,¹ and Bai-Xiang Xu¹

Institute of Materials Science, Technische Universität Darmstadt, Germany

(Dated: 3 September 2022)

The influence of defect dipoles on the electrocaloric effect (ECE) in acceptor doped BaTiO_3 is studied by means of lattice-based Monte-Carlo simulations. An effective Hamiltonian is used, which includes a Landau-type on-site energy term, a dipole-dipole interaction energy, a domain wall energy and an electrostatic energy describing the coupling to the external electric field. Oxygen vacancy-acceptor associates are described by fixed defect dipoles with orientation parallel or anti-parallel to the external field. By a combination of canonical and microcanonical simulations the electrocaloric effect is directly evaluated. Our results show that in the case of anti-parallel defect (APD) dipoles the ECE can be positive or negative depending on the density of defect dipoles. Moreover, a transition from a negative to positive ECE can be observed for a relatively high density of APD dipoles when the external field increases. These transitions are due to the delicate interplay of internal and external fields and can be explained from the analysis of the domain structure evolution and related field-induced entropy changes.

Ferroelectric materials based on BaTiO_3 are of interest for solid state refrigeration because of their significant electrocaloric effect.^{1–5} Moya *et al.*² measured the ECE of single crystalline BaTiO_3 samples in the direct and indirect way and reported around 1 K temperature variation. Qian *et al.*⁶ investigated the ECE in $\text{BaZr}_{0.2}\text{Ti}_{0.8}\text{O}_3$ and found a large temperature variation of 4.5 K over a 30 K operating temperature range, which is wider than that in BaTiO_3 . Recently, experimental^{7–9} and theoretical^{10,11} studies revealed the coexistence of the positive ($\Delta T > 0$) and negative ($\Delta T < 0$) ECE under applied electric field. The negative ECE is expected if the polarization at lower temperature is smaller than at higher temperature. If the applied field is not collinear with the dielectric polarization of the material, the applied field may increase the amount of dipolar entropy and thus reduce the phonon contribution under iso-entropic conditions causing a negative ΔT . Pirc *et al.*¹² studied the negative ECE for an anti-ferroelectric materials based on a generic Kittel model and found transitions from a negative to a positive ECE depending on the applied field below the Curie temperature. Axelsson *et al.* modeled the ECE by directly evaluating the entropy from the partition function of an one-dimensional lattice model¹³ and showed how the field applied along a particular lattice direction induces a negative ECE. According to their model the sign reversal of ECE requires two phase transitions close in temperature. Also Ponomareva and Lisenkov¹⁰ found that by varying the direction and strength of the applied field the sign of the ECE can be efficiently controlled.

While the influence of phase transitions on the ECE in ferroelectrics and ferroelectric relaxors is widely studied, much less is known on the role of dopants.

In acceptor doped material Ba or Ti/Zr ions are substituted by ions with a lower valence. In this case, charge

neutrality is typically obtained by compensating oxygen vacancies. Acceptor doped materials, which are also referred to as hard doped, are difficult to polarize, exhibit high coercive fields as well as small strains.¹⁴ It is well established that in acceptor doped materials defect reactions between dopant and oxygen vacancies can occur. For BaTiO_3 it was demonstrated that $(\text{Mn}_{\text{Ti}}'' - \text{V}_{\text{O}}^{\bullet\bullet})^\times$ associates with an excess orientation parallel to the spontaneous polarization are present in reduced crystals.¹⁵ Non-switching defect dipoles impose a restoring force for reversible domain switching¹⁶ and thus might have an impact on the ECE, since their gradual re-orientation is determined by the barrier for oxygen vacancy migration, whence these defect complexes cannot immediately follow the polarization switching.¹⁷ The possibility to enhance and control the ECE in dielectric materials by the presence of internal dipoles was formulated by Van Vechten¹⁸ in an US-patent in the late seventies. Only recently, however, Grünebohm *et al.*¹⁹ showed by means of MD simulations using an effective Hamiltonian approach that the ECE can switch in the presence of fixed defect dipoles from positive to negative behavior. In this study, we analyze the impact of fixed parallel and APD dipoles on the ECE by directly simulating the adiabatic temperature changes in lattice-based Monte-Carlo simulations using a recently developed Hamiltonian for BaTiO_3 .²⁵ We specifically address the transition from a negative to positive ECE as a function of temperature, field strength and defect concentration in the presence of defect dipoles that induce an inhomogeneous electric field. The model contains a Landau-type on-site energy term E_D , a dipole-dipole interaction energy E_{dip} , the domain wall energy E_{gr} that arises from short-range and elastic interactions²¹, and the electrostatic energy E_e , and is extended by lattice sites with fixed non-switchable polarization to mimic the presence of defect dipoles. The elastic energy and the electrostrictive interaction are not explicitly included in the Hamiltonian²², but the elastic energy contribution to domain wall energies is implicitly

^{a)} Electronic mail: y.ma@mfm.tu-darmstadt.de

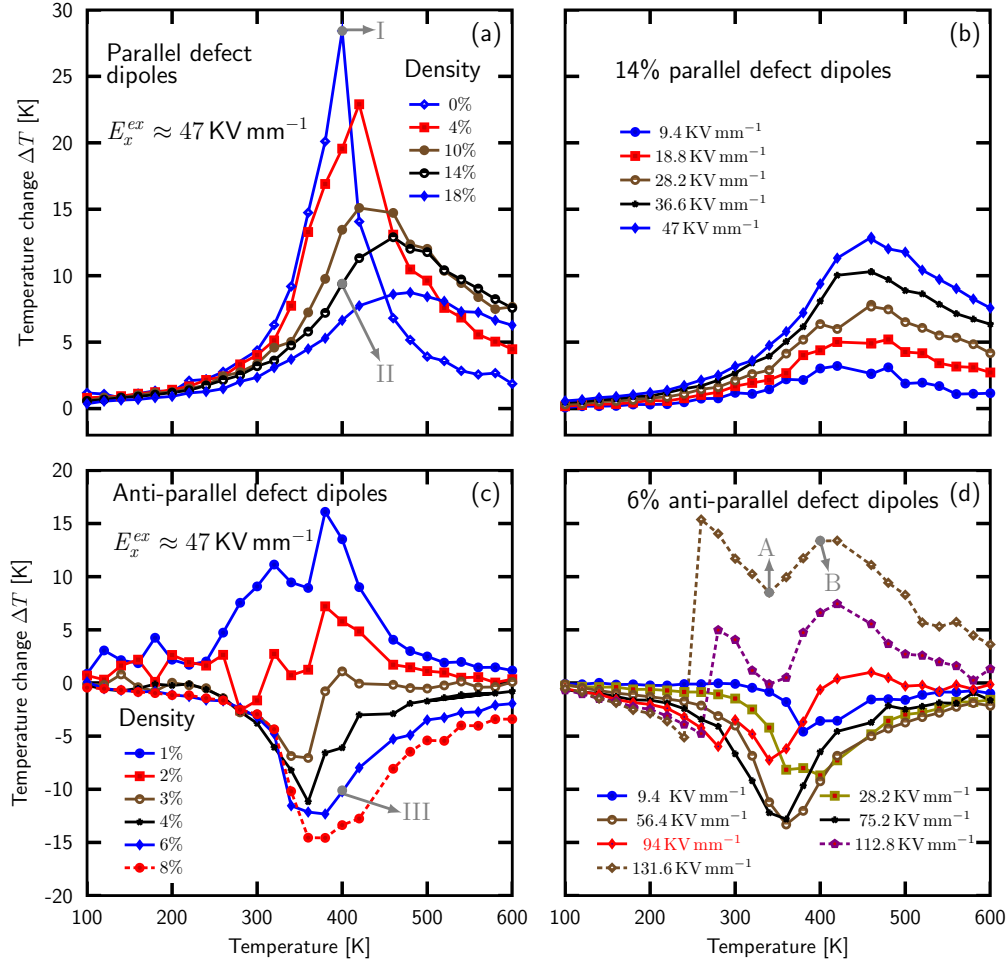


FIG. 1. Positive and negative ECE. (a) ECE in the presence of collinearly aligned parallel defect dipoles. Different defect concentrations are considered under a given external field. (b) ECE as a function of the external field for a defect concentration of 14%. (c) Positive and negative ECE in presence of APD dipoles. When the defect density exceeds a critical value, the resultant internal anti-parallel field overcomes the external field and negative temperature change is observed (negative ECE). (d) Influence of the external field, while APD dipoles with a concentration of 6% are present. When the external field surpasses the internal field induced by the APD dipoles, negative ECE appears only at low temperature region, while positive ECE dominates at higher temperature.

considered in the gradient term. We expect that this simplification has no qualitative influence on the calculated entropy variations, since defect dipoles have only a weak elastic strain field and the possible impact of elastic energies on the domain switching behavior is the same in the isothermal and adiabatic configurations with applied field.

Since the orientation of defect dipoles follows the spontaneous polarization only on time scales of days to months depending on temperature and is one reason for aging in a poled material, the simplifying assumption of a fixed dipole orientation within an ECE cycle occurring on much shorter time scales is reasonable. Such unidirectional defect dipoles might be introduced through a long-time poling process.^{23,24} Different types of defect dipoles are investigated, namely defect dipoles pointing parallel to \mathbf{E}^{ex} and defect dipoles oriented anti-parallel

to \mathbf{E}^{ex} . The local polarization for the defects is assumed as 0.46 C m^{-2} , and the direction of these defect dipoles is fixed. When several lattice sites are occupied by one type of defect dipole, i.e. the parallel or APD dipoles, this internal field becomes stronger or inhomogeneous, respectively. Thus, an impact on the accessible entropy changes can be expected.

The influence of the concentration of parallel defect dipoles on the ECE is illustrated in Fig. 1(a). For pure BaTiO₃ the magnitude of $\Delta T/\Delta E$ at the peak is comparable with the experimental data ($0.57 \times 10^{-6} \text{ K m/V}$ vs. $0.83 \times 10^{-6} \text{ K m/V}$).² With increasing defect concentration, the ECE peak decreases and the maximum is shifting to higher temperatures due to the internal field induced by the defect dipoles. By contrast, the obtainable ECE is enhanced when the external field is increased (see Fig. 1(b)) since the higher external field can change

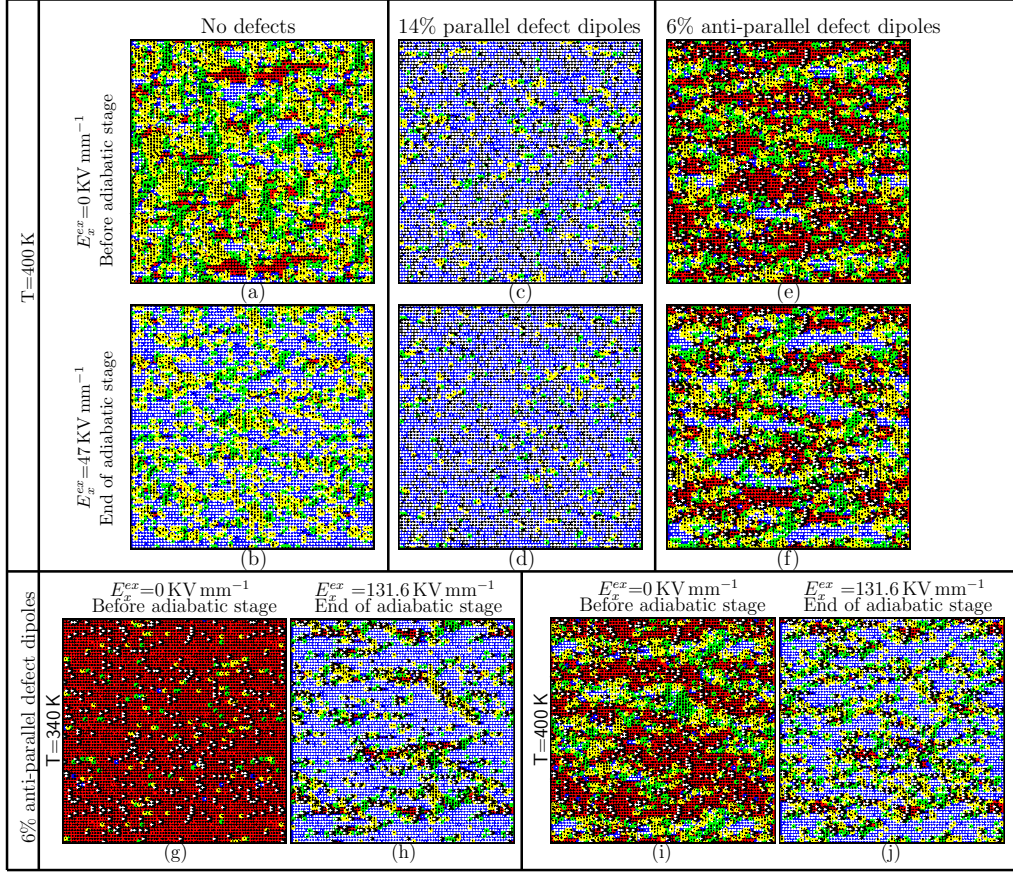


FIG. 2. Domain structure explanation of ECE for the points I, II, III, A and B marked in Fig. 1. The external field is applied in the horizontal direction and points to the right. (a) and (b) are the domain structure snapshots before and after the adiabatic stage for the point I; (c) and (d) for point II; (e) and (f) for point III; (g) and (h) for point A; (i) and (j) for point B. The black dots with white arrows represent the defect dipoles, either parallel or anti-parallel to the external field. The red, blue, yellow and green dots represent the dipoles pointing respectively to the left, to the right, to the top and to the bottom.

the extent of the order more severely.

After the initial poling procedure the ideal sample shows a multiple domain configuration (Fig. 2(a)), which is switched into a state of reduced dipolar entropy (Fig. 2(b)) and thus increased temperature under adiabatic conditions by an external field. It can clearly be seen that a smaller number of domains occurs in the presence of the external field than in the pre-poled sample without external field. If we compare now with the case, where defect dipoles in collinear orientation to the external field are present, the situation is changing. In the initial state the configurational space is reduced as compared to the defect free sample (see Fig. 2(a) and (c)), since defect dipoles are creating an internal field that is locally stabilizing the domain structure against thermal fluctuations. If the external field is now switched on, the change in configurational entropy (S_{conf}) is smaller than in the defect-free case and thus a smaller temperature variation is possible, which is explaining the field dependence of the ECE. If fewer domain walls disappear, the decrease of the domain wall energy is reduced and the excess heat is reduced.

A different scenario occurs, if the defect dipoles are pre-aligned in anti-parallel direction; a situation which can be installed by poling the sample on extended time scales, before reversing the field direction. For defect concentrations above 3% the ECE is turning from a positive effect into negative direction and becomes more pronounced with increasing external field. This can be explained again from the characteristic domain structure shown in Fig. 2(e) and (f). Initially, the system is close to a single domain configuration (Fig. 2(e)) in orientation parallel to the defect dipoles and thus has a small S_{conf} because of the large internal field $\langle \mathbf{E}_i \rangle = -80.0 \text{ KV mm}^{-1}$.

If now an external field of $\mathbf{E}^{ex} = 47.0 \text{ KV mm}^{-1}$ is switched on, the internal field is partly compensated and the material can locally sample a multi-domain structure with increased S_{conf} (see Fig. 2(f)) corresponding to a reduced potential energy. Thus, entropy has to be removed from the phonons under iso-entropic conditions and the negative ECE appears. It should be noted that the domain snapshots, i.e. Fig. 2(e) and (f), are for 400 K. At the negative ECE peak, i.e. 380 K, the prepoled sample is more like a single domain type, and the S_{conf} change

is more prominent.

When the magnitude of \mathbf{E}^{ex} (e.g. 94 KV mm^{-1}) is, however, higher than that of the internal field, both the ECE and the negative ECE start to coexist. A sharp rise in temperature is observed at the transition from the negative into positive temperature change, and both the negative ECE peak and the first positive ECE peak shift to lower temperature with increasing \mathbf{E}^{ex} . This transition, again, can be explained by inspecting the domain structure for the case $\mathbf{E}^{ex} = 131.6 \text{ KV mm}^{-1}$. Before the external field is applied, thermal energy fluctuations provide the ability to sample configurational space in areas, which are not pinned by the presence of local defect dipoles. This can be seen in Fig. 2(g), where the single domain states (red) form a percolating (non switching) network of the sites localized in the direct vicinity of dipoles, while multiple domain configurations, which can take various iso-energetic configurations, occur in between. If now a very high external field \mathbf{E}^{ex} is switched on, the situation is reversing and sites being part of the initially inactive percolating network around the APD sites (see Fig. 2(h)) are those where the external field is compensated. Thus, only these sites in the direct vicinity of defect associates can effectively sample configurational space, while the remaining matrix atoms orient parallel to the external field and do not contribute to S_{conf} . Since the relative number of sites which can possibly flip their configuration scales is scaling with the defect concentration and is thus smaller than the number of sites dominated by the external field, the S_{conf} is reduced and the ECE becomes positive again. The initially disordered sites are realigned parallel to the electric field and the total potential energy varies sharply. With increasing initial temperature this local order is further reduced and the material behaves like a regular ferroelectric material. If the initial temperature is further increased, the temperature variation is showing a cusp and a hump at about $T = 340 \text{ K}$ in Fig. 1(d). This double-peak behavior can be attributed to a temperature induced phase transition in the initial state. As can be seen from the domain configuration, the local domains have formed at $T = 400 \text{ K}$ and the system has locally taken a multi-domain configuration in the initial prepoled sample, which is higher in potential energy than the single domain case prevailing below $T = 340 \text{ K}$. Thus the effective ΔT is raising again.

The high applied field is reasonable, since the simulated sample size 25.2 nm^2 is within the ultra-thin film regime.^{25,26} Due to the high external field, a high concentration of APD dipoles is expected to generate high enough anti-parallel internal field to reverse the ECE sign. In samples with bigger size or polycrystalline materials, the external field and the defect concentration is much smaller (e.g. 1.0% defects under 7.83 KV mm^{-1} through linear interpolation as indicated in Fig.S2 of Supplementary material)²⁰. Additionally, the sample with high density of the defect dipoles can be synthesized, e.g. $\text{Ba}(\text{Ti}_{0.93}\text{Fe}_{0.07})\text{O}_3$.²⁷

In summary, our results reveal that the ECE of BaTiO_3 can be tuned by the presence of defect dipoles due to

acceptor-vacancy associates, which agrees qualitatively with the MD results¹⁹. The APD dipoles act as "memory elements" which reduce the configurational space in the prepoled sample and thus allow to turn the positive ECE into a negative ECE. Under certain fields both effects can be combined, which offers possibilities to increase the cooling efficiencies of electrocaloric devices (see Supplementary material)²⁰, and indicates potential applications of ferroelectric materials with defect dipoles for the ECE.

The funding of Deutsche Forschungsgemeinschaft (DFG) SPP 1599 B3 (XU 121/1-1, AL 578/16-1) is gratefully acknowledged.

- ¹Y. Bai, X. Han, and L. Qiao, Appl. Phys. Lett. **102**, 252904 (2013).
- ²X. Moya, E. Stern-Taulats, S. Crossley, D. González-Alonso, S. Kar-Narayan, A. Planes, L. Mañosa, and N. D. Mathur, Adv. Mater. **25**, 1360 (2013).
- ³H. Maiwa, Ferroelectrics **450**, 84 (2013).
- ⁴G. Singh, I. Bhaumik, S. Ganesamoorthy, R. Bhatt, A. K. Karnal, V. S. Tiwari, and P. K. Gupta, Appl. Phys. Lett. **102**, 082902 (2013).
- ⁵H.-J. Ye, X.-S. Qian, D.-Y. Jeong, S. Zhang, Y. Zhou, W.-Z. Shao, L. Zhen, and Q. M. Zhang, Appl. Phys. Lett. **105**, 152908 (2014).
- ⁶X.-S. Qian, H.-J. Ye, Y.-T. Zhang, H. Gu, X. Li, C. A. Randall, and Q. M. Zhang, Adv. Funct. Mater. **24**, 1300 (2014).
- ⁷J. Peräntie, J. Hagberg, A. Uusimäki, and H. Jantunen, Phys. Rev. B **82**, 134119 (2010).
- ⁸Y. Bai, G.-P. Zheng, and S.-Q. Shi, Mater. Res. Bull. **46**, 1866 (2011).
- ⁹S. Uddin, G.-P. Zheng, Y. Iqbal, R. Uvic, and J. Yang, J. Appl. Phys. **114**, 213519 (2013).
- ¹⁰I. Ponomareva and S. Lisenkov, Phys. Rev. Lett. **108**, 167604 (2012).
- ¹¹B. Li, J. B. Wang, X. L. Zhong, F. Wang, Y. K. Zeng, and Y. C. Zhou, Europhys. Lett. **102**, 47004 (2013).
- ¹²R. Pirc, B. Rožič, J. Koruza, B. Malič, and Z. Kutnjak, Europhys. Lett. **107**, 17002 (2014).
- ¹³A.-K. Axelsson, F. Le Goupil, L. J. Dunne, G. Manos, M. Valant, and N. M. Alford, Appl. Phys. Lett. **102**, 102902 (2013).
- ¹⁴B. Jaffe, W. Cook, and H. Jaffe, *Piezoelectric ceramics* (Academic, London, UK, 1971).
- ¹⁵G. H. Jonker and P. V. Lambeck, Ferroelectrics **21**, 641 (1978).
- ¹⁶X. Ren, Nat. Mater. **3**, 91 (2004).
- ¹⁷P. Erhart, P. Träskelin, and K. Albe, Phys. Rev. B **88**, 024107 (2013).
- ¹⁸J. Van Vechten, "Dielectric refrigerator using orientable defect dipoles," (1979), US Patent 4,136,525.
- ¹⁹A. Grünebohm and T. Nishimatsu, "Influence of defects on the ferroelectric and electrocaloric properties of BaTiO_3 ," (2015), arXiv:1502.05201v1.
- ²⁰"See supplemental material at [url] for details of model."
- ²¹T. Nishimatsu, U. V. Waghmare, Y. Kawazoe, and D. Vanderbilt, Phys. Rev. B **78**, 104104 (2008).
- ²²B. L. Li, X. P. Liu, F. Fang, J. L. Zhu, and J.-M. Liu, Phys. Rev. B **73**, 014107 (2006).
- ²³L. Zhang, E. Erdem, X. Ren, and R.-A. Eichel, Appl. Phys. Lett. **93**, 202901 (2008).
- ²⁴C. M. Folkman, S. H. Baek, C. T. Nelson, H. W. Jang, T. Tybell, X. Q. Pan, and C. B. Eom, Appl. Phys. Lett. **96**, 052903 (2010).
- ²⁵Y.-B. Ma, K. Albe, and B.-X. Xu, Phys. Rev. B **91**, 184108 (2015).
- ²⁶R. Gaynudinov, M. Minnekaev, S. Mitko, A. Tolstikhina, A. Zenkevich, S. Ducharme, and V. Fridkin, JETP Lett. **98**, 339 (2013).
- ²⁷F. Lin and W. Shi, Physica B **407**, 451 (2012).